ISME

ARTICLE

Spatial regulation of cell motility and its fitness effect in a surface-attached bacterial community

Emrah Şimşek [1,5,6], Emma Dawson[1,6], Philip N. Rather[2,3,4] and Minsu Kim [1,2 ✉]

On a surface, microorganisms grow into a multi-cellular community. When a community becomes densely populated, cells migrate away to expand the community's territory. How microorganisms regulate surface motility to optimize expansion remains poorly understood. Here, we characterized surface motility of *Proteus mirabilis*. *P. mirabilis* is well known for its ability to expand its colony rapidly on a surface. Cursory visual inspection of an expanding colony suggests partial migration, i.e., one fraction of a population migrates while the other is sessile. Quantitative microscopic imaging shows that this migration pattern is determined by spatially inhomogeneous regulation of cell motility. Further analyses reveal that this spatial regulation is mediated by the Rcs system, which represses the expression of the motility regulator (FlhDC) in a nutrient-dependent manner. Alleviating this repression increases the colony expansion speed but results in a rapid drop in the number of viable cells, lowering population fitness. These findings collectively demonstrate how Rcs regulates cell motility dynamically to increase the fitness of an expanding bacterial population, illustrating a fundamental trade-off underlying bacterial colonization of a surface.

The ISME Journal; https://doi.org/10.1038/s41396-021-01148-w

INTRODUCTION

In nature, bacteria often grow on a surface and develop a multi-cellular community [1, 2]. When a community becomes densely populated, cells migrate away to expand their community [3]. This process poses significant industrial and medical challenges because it leads to the spread of biofouling and chronic infections [4–6]. However, several fundamental questions remain unanswered. Specifically, dispersal is mediated by phenotypic (or genotypic) "variants" [7]. What are the ecological factors that drive the generation of these migratory variants? What are the signal transduction pathways that are used to sense these ecological factors and trigger the generation of migratory variants?

The importance of understanding migration extends beyond microorganisms because migration is a fundamental process of living organisms [8, 9]. Migration results in a profound change in population density in space and time, altering local ecological interactions, e.g., species competition and spread of invasive species [10–15]. A wide variety of organisms exhibit partial migration, where a fraction of a population moves away while the rest remains sessile. This type of migration has been documented for mammals, birds, fish, amphibians, and insects [16]. However, how and why a population diversifies when expanding its territory is poorly understood. While several theoretical studies have proposed potential benefits of partial migration [17–19], they have not been experimentally tested.

In this study, we characterized the surface expansion of bacterial communities in the context of partial migration. We chose *Proteus mirabilis* as a model system because of its superior ability to expand its community [20]. This superior ability underlies the pathogenesis of this bacterium as it enables *P. mirabilis* cells to reach across the urethra and colonize the bladder and kidneys and leads to rapid surface fouling of newly inserted catheters [21–25]. *P. mirabilis'* superior expansion can be visualized on agar surfaces in a laboratory, as its colony can expand on high agar concentrations (>1%), which are too stiff for other model bacteria including *Escherichia coli* or *Bacillus subtilis* [9, 26–28]. Here, we investigated the expansion dynamics of *P. mirabilis* to identify a regulatory mechanism and strategy for its surface colonization.

MATERIALS AND METHODS

Bacterial growth conditions

P. mirabilis ATCC 7022 and its derivatives were used (Supplementary Tables 1 and 2). Liquid cultures were prepared in Luria-Bertani (LB) broth at 37 °C with shaking at 200 rpm. Cells were inoculated from an −80 °C frozen stock a day before an experiment and grown overnight. A small volume of an overnight culture was suspended in fresh medium to prepare an experimental culture. Cells were grown in an experimental culture for at least five doublings before measurements were made as described in the text. Cell density was determined by quantifying the optical density at 600 nm wavelength (OD_{600}) using a Genesys20 spectrophotometer (Thermo Fisher) with a standard cuvette (16.100-Q-10/Z8.5; Starna Cells).

Microscopy and image analysis

The cells were imaged using an inverted microscope (Olympus IX83P2Z). The microscope was controlled by the MetaMorph software (Molecular Devices) and housed in a microscope incubator (InVivo Scientific), which

[1]Department of Physics, Emory University, Atlanta, GA 30322, USA. [2]Graduate Division of Biological and Biomedical Sciences, Emory University, Atlanta, GA 30322, USA. [3]Department of Microbiology and Immunology, Emory University, Atlanta, GA 30322, USA. [4]Research Service, Atlanta VA Medical Center, Decatur, GA 30033, USA. [5]Present address: Department of Biomedical Engineering, Duke University, Durham, NC 27708, USA. [6]These authors contributed equally: Emrah Şimşek, Emma Dawson. ✉email: minsu.kim@emory.edu

maintained the temperature of samples at 37 °C during the experiments. Images were captured using a Neo 5.5 scientific CMOS camera (Andor). Images were analyzed using MicrobeJ, a freely available plug-in for ImageJ, or custom-built MATLAB software. Additional details about the experiments and analyses are provided in Supplementary Information.

RESULTS

Expansion dynamics of a surface-attached *P. mirabilis* colony

We studied the expansion of a wild-type (WT) *P. mirabilis* population by depositing an inoculum droplet on a surface of an LB medium solidified with ~2% agar. When deposited on a surface, a WT *P. mirabilis* population first grows in its original inoculum zone and forms a colony (Supplementary Fig. 1a). Only after a colony reaches a high cell density (~10^9 cells/cm^2), it initiates migration (Supplementary Fig. 1b). Migration is visualized by the appearance of a faint halo beyond the distinct boundary of a densely-packed parental colony (Fig. 1A). Throughout population migration, the boundary of the parent colony remains stationary and distinct, suggesting that a majority of cells remain in the parental colony.

We then directly determined the migrating fraction in a colony. *P. mirabilis* cells migrate on stiff surfaces by differentiating to an hyperelongated and hyperflagellated phenotype [20]. Cells exhibiting this motile phenotype can migrate across a surface through a process known as swarming [9, 26–29]. We and others have shown that differentiation occurs in a subpopulation of cells [30, 31]. Here, we quantified the fraction of this subpopulation by harvesting the entire population and determining the number of hyperelongated cells with a microscope (Supplementary Fig. 2). We found that only ~1% of cells exhibited the motile phenotype (Fig. 1C, green).

Severe repression of migration in the inner region of an expanding colony

How and why is the migratory fraction kept at such a low level? We first sought to unravel a regulatory mechanism controlling the migratory fraction by characterizing the spatio-temporal dynamics of the motile phenotype. The *flhDC* gene encodes the master regulator for differentiation into the motile phenotype [32, 33]. We constructed a transcriptional fusion of the *flhDC* and green fluorescent protein (*gfp*) genes and tracked *flhDC* expression by monitoring GFP intensity in a colony over time. We found that as a colony matures, GFP intensity increases in cells at the colony edge (Supplementary Movie left panel). These GFP-bright cells differentiate to the motile phenotype and migrate away from the parental colony. In the inner region of the colony, however, GFP intensity remained low, and no differentiation occurred (Supplementary Movie right panel). This severe repression of motility in the inner region explains how a large fraction of a population remains sessile in an expanding colony.

Additionally, we found that there was a narrow, distinct band of cells at the edge of the colony which comprised most GFP-bright cells (Supplementary Movie left panel). The formation of this band can be described by the coffee ring effect, a well-known physical phenomenon caused by capillary flow which pushes particles to the edge of a liquid droplet [34]. This effect was also frequently observed in previous studies of bacterial colony formation [35, 36]. We wondered whether the formation of this band is responsible for the preferential increase in GFP intensity at the colony edge. To avoid this effect, we started colonies from single cells by diluting and spreading an inoculum droplet over a large area of agarose surface. Colonies originating from single cells did not exhibit such bands, and yet GFP intensity was still preferentially higher at the colony edge (Fig. 2A top panel, and Supplementary Fig. 3). To quantify this inhomogeneity, we determined the radial distribution of the bright pixels across multiple colonies. We first
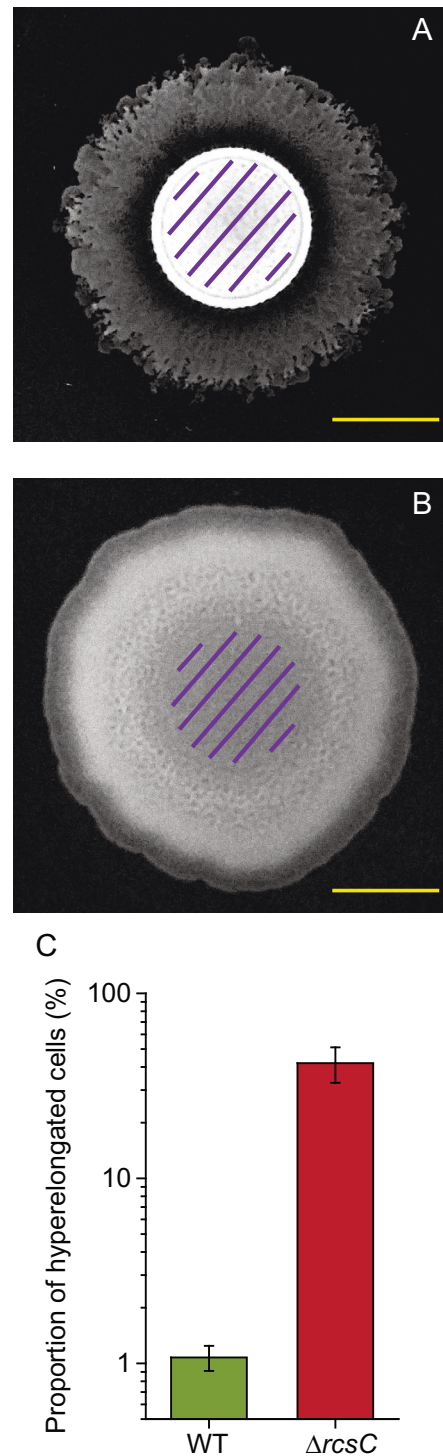
Fig. 1 Different migration pattern of WT and Δ*rcsC* strains. A WT colony 7 h after inoculation on a LB agar surface. **B** Δ*rcsC* colony 6 h after inoculation. Note that a Δ*rcsC* colony begins colony expansion ~1 h earlier than a WT colony. Purple-line zones indicate the original inoculum area. **C** Migratory cells as a proportion of all cells in the colony. Colonies expanding on agar surfaces were suspended in liquid LB culture, and the cells (from the colonies) were immediately imaged with a microscope. Cells were counted and hyperelongated cells (swarmers) were identified (Supplementary Fig. 2). *p* value (from a T-test) = 0.00069. Error bars indicate one standard deviation from two independent experiments. ~800 cells were analyzed in each experiment. Scale bars represent 10 mm.
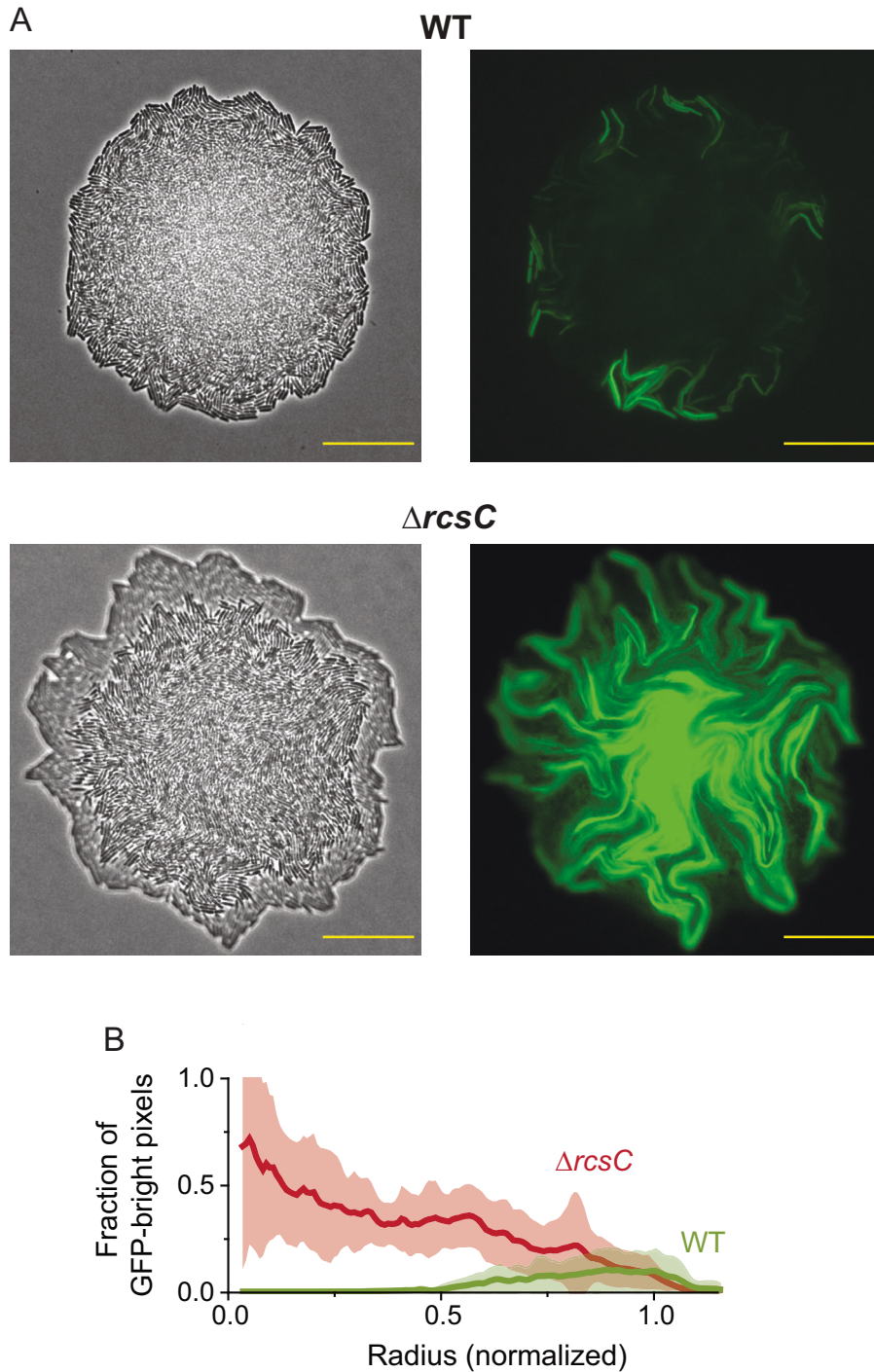
Fig. 2 Spatially inhomogeneous motility pattern. A Phase contrast and fluorescence images of WT and ΔrcsC micro-colonies. A P$_{flhDC}$ − *gfp* transcriptional fusion construct was used. The ΔrcsC images show a colony right before the onset of migration. The WT images show a colony in a similar size. Note that WT colonies initiate migration at a larger colony size than ΔrcsC colonies (Supplementary Fig. 9). WT colonies right before the onset of migration (which are larger than what is shown here) exhibit similar, spatially inhomogeneous distribution of GFP intensities (Supplementary Fig. 3). **B** Radial distribution of GFP-bright pixels right before the onset of migration. Each colony was divided into 125 rings of equal radial width. GFP-bright pixels (whose GFP intensities were above the threshold as discussed in the main text) were identified, and the fraction of these pixels within each ring (i.e., the number of GFP-bright pixels divided by the total number of pixels within each ring) is plotted as a function of radial position. Here, the radius of each ring was normalized to the actual radius of the colony; absolute (unnormalized) ring radius was also considered (Supplementary Fig 4). Here, the distribution extends slightly beyond one in the x-axis because of ruggedness of colony perimeter. 1 pixel corresponds to 0.1083 μm. The filled areas represent the standard deviation from 10 colonies. Scale bars represent 30 μm.

characterized the minimum fluorescence threshold value for differentiation into the motile phenotype, which revealed that the cells that expressed fluorescence values greater than 560 (a.u.) eventually differentiated and swarmed. We then determined the radial distribution of the pixels whose GFP intensities were above the threshold as a function of both the normalized (Fig. 2B green) and unnormalized (Supplementary Fig. 4 green) radius. The fraction of GFP-bright pixels within a half the colony radius is

almost zero, again showing that GFP-bright cells are primarily located at the colony edge.

The *rcs* mutant exhibits very different migration dynamics
In the WT strain, the boundary of a parental colony remains stationary and distinct during expansion (Fig. 1A), because a majority of cells do not participate in migration (Fig. 1C). Our microscope experiments attribute this low participation to severe repression of *flhDC* expression in the colony center (Fig. 2). During our transposon mutagenesis screening, we identified mutants that showed different dynamics of colony expansion: they shifted the entire colony boundary outward during migration (Fig. 1B and Supplementary Fig. 5). We found that these mutants have the transposon insertion in the *rcsC* or *rcsB* genes, two components of the Rcs phosphorelay system [37–39]. As transposon insertion might be unstable, we performed clean knockouts of these genes (Supplementary Methods). These mutants exhibited the same, outward shift of the colony boundary. We next tracked the radius

of the population edge, which showed that the edge moves faster in the mutant colony than in a WT colony (Supplementary Fig. 6).

The rapid expansion of the colony boundary exhibited by the mutants suggests that a large fraction of the population migrates. We confirmed this by quantifying the fraction of cells expressing the motile phenotype in a Δ*rcsC* population. We found that ~50% of a population participates in migration (Fig. 1C, red), a fraction significantly higher than the ~1% observed in the WT population (Fig. 1C, green). Importantly, this large increase in the migratory fraction indicates that the *rcsC* knockout relieved the repression of the master regulator gene *flhDC* expression. If so, because the repression occurred mostly in the colony center in the WT, Δ*rcsC* colonies would exhibit strong *flhDC* expression in the colony center. This prediction is supported by our microscope images, which showed high GFP intensities in the center of Δ*rcsC* colonies (Fig. 2A bottom panel). This can be seen in the radial distribution of GFP-bright pixels as well, which shows that the fraction of GFP-bright pixels is higher in the colony center than the edge (Fig. 2B,
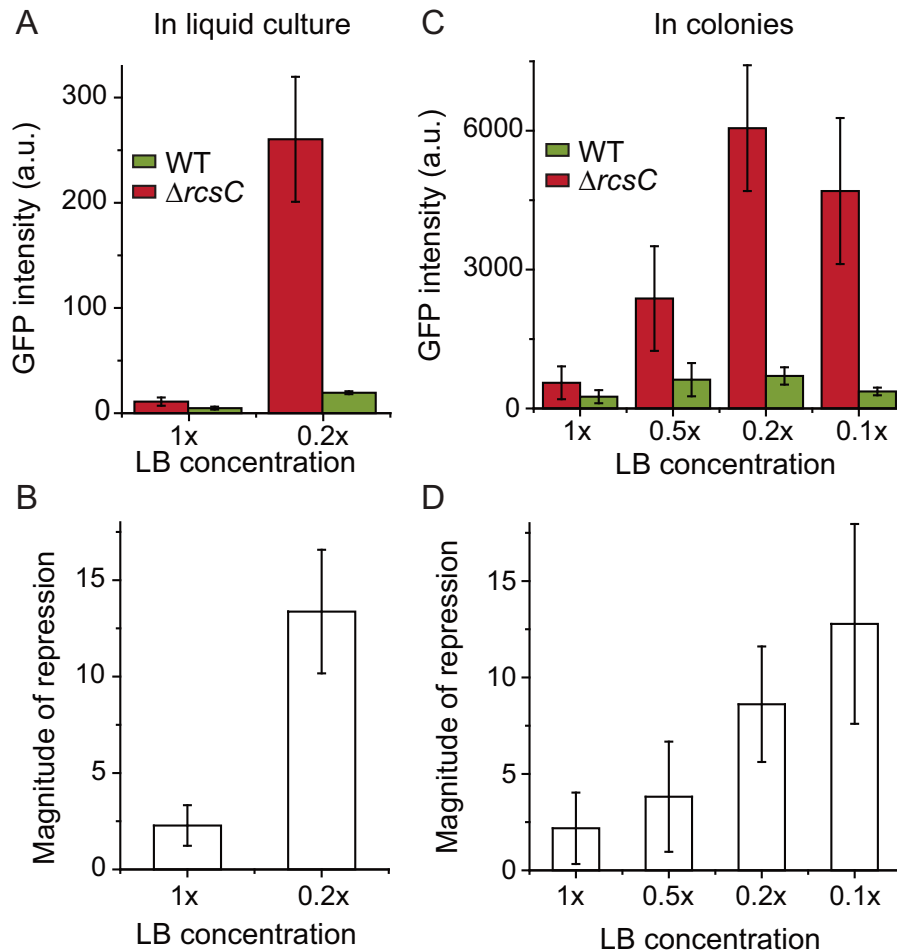

Fig. 3 P*flhDC* – *gfp* expression in liquid cultures and micro-colonies. A *flhDC* expression in liquid cultures. Cells were grown in liquid culture to an OD_{600} of 0.35, transferred to a coverslip, and imaged with a microscope. GFP intensities in ~100 individual cells were measured and averaged in each condition. Error bars represent the standard deviation of two independent experiments. *p* value (from a T-test) = 0.064 for 1× and 0.015 for 0.2× LB. **B** Magnitude of *flhDC* repression by Rcs in liquid cultures. The magnitude of repression was determined by dividing the GFP intensity of Δ*rcsC* by that of WT (Fig. 3A). Repression is more severe in lower nutrient conditions. *p* value (from a T-test) = 0.075 for 1× and 0.038 for 0.2× LB. **C** *flhDC* expression in the colony center right before the onset of colony migration. The GFP intensity within a 100 pixel (~10 µm) circle was measured at the moment of colony expansion and averaged over 10 colonies (Supplementary Fig. 7). Error bars represent the standard deviation of the average GFP intensity from two independent experiments. **D** Magnitude of *flhDC* repression by Rcs in colonies right before the onset of colony migration. The magnitude of repression was determined by dividing the GFP intensity of Δ*rcsC* by that of WT (Fig. 3C). We additionally determined the magnitude of repression at various points during the colony development for 1× and 0.2× LB (Supplementary Fig. 11).

red). Our observation of *flhDC* repression by Rcs is consistent with our and others' previous findings that *flhDC* is a member of a large Rcs regulon [37–43]. However, regulation of *flhDC* expression is complex, and exactly how Rcs affects *flhDC* expression was not clear.

Nutrient-dependent repression of cell motility by Rcs

One major difference between cells in the colony center and edge is the access to nutrients; because nutrients diffusing into the colony are first utilized by cells in the edge, less nutrients are accessible to cells in the colony center [44–48]. Therefore, one possible explanation for low *flhDC* expression in the WT colony center is that its expression is repressed under low-nutrient conditions. Importantly, given our finding above that Rcs mediates the repression, this would mean that the repression of *flhDC* expression by Rcs is nutrient-dependent. To examine this possibility, we compared the magnitude of *flhDC* repression under different nutrient levels. We first measured the *flhDC* expression in WT and $\Delta rcsC$ cells at two different nutrient levels ($1\times$ and $0.2\times$ LB) in liquid cultures. An advantage of a liquid culture is that it can be shaken and well-mixed, providing better control for a nutrient condition. Also, because cell density in a liquid culture can be easily determined, *flhDC* expression can be compared at the same cell density. Cells were grown to an OD_{600} of 0.35 in liquid culture, transferred to a coverslip, and imaged with a microscope. We found that *flhDC* expression in WT cells was lower than that in $\Delta rcsC$ cells in both nutrient conditions, which is consistent with the observed repressive effect of Rcs on *flhDC* expression. We then calculated the magnitude of repression by dividing the GFP intensity of $\Delta rcsC$ by that of WT (Fig. 3B and Supplementary Fig. 7). We found that the repression was much more severe in $0.2\times$ LB than $1\times$ LB.

Because our other measurements focused on the center of colonies growing on a semi-solid surface (rather than liquid cultures), we repeated our previous agarose experiments with different LB concentrations and compared the magnitude of *flhDC* repression in the colony center. The *flhDC* expression can vary from cell-to-cell (Fig. 2A; further discussed in *Discussion*). Our analysis showed that averaging *flhDC* expression within a small disk of radius $\sim 10\,\mu m$ (which corresponds to the width of a few cells) is sufficient to average out this variation (Supplementary Fig. 8). We found that the averaged *flhDC* expression in the colony center is always lower in the WT than in the $\Delta rcsC$ strain in all nutrient conditions tested ($1\times$, $0.5\times$, $0.2\times$ and $0.1\times$ LB), again showing *flhDC* repression by Rcs (Fig. 3C). Importantly, the magnitude of repression increased as the nutrient level decreased (Fig. 3D). Here, this comparison was made for the colonies at the onset of colony migration, but this onset occurred at different colony sizes under different nutrient levels (Supplementary Fig. 9). Thus, we also determined the repression for a smaller but uniform colony size ($20\,\mu m$ radius), which again showed stronger *flhDC* repression at lower nutrient levels (Supplementary Figs. 10 and 11). This finding agrees with our liquid culture data and further supports that Rcs-mediated repression of *flhDC* expression is nutrient-dependent.

Fitness advantage of the WT (*rcsC*+) strain

A $\Delta rcsC$ colony expands faster than a WT colony (Supplementary Fig. 6), because it has a much higher fraction of migratory cells (Fig. 1C). Then, what is the advantage of keeping the migratory fraction low? To address this question, we compared the fitness of WT and $\Delta rcsC$ strains. Specifically, we spread cells on an agar surface and evaluated the biomass yield by measuring $OD_{600} \times ml$ and cell viability by counting colony forming units (CFU) over time. We used $0.2\times$ LB agar because the repression is pronounced in a low-nutrient environment (Fig. 3C). We found that the $\Delta rcsC$ strain produced less biomass than WT in a given territory, although the difference is marginal (Fig. 4A, circles and squares). Importantly,
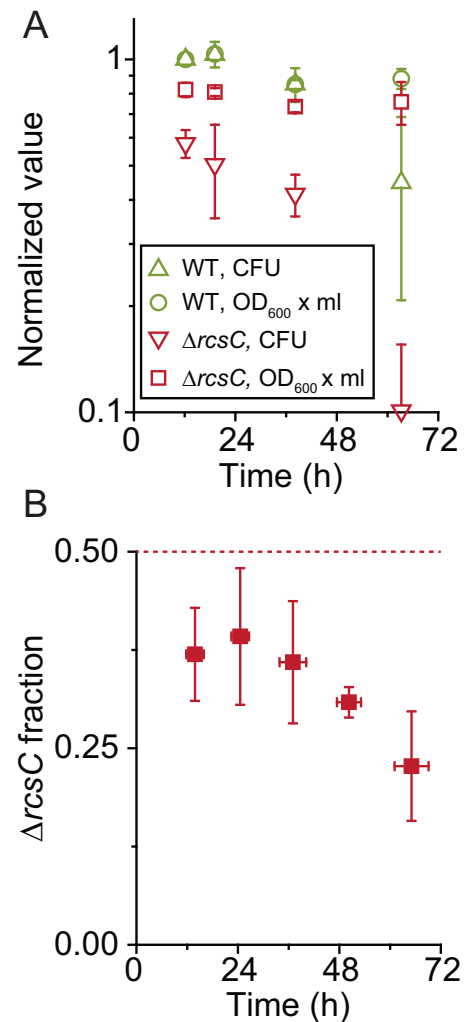

Fig. 4 The fitness effect of Rcs. A Biomass ($OD_{600} \times ml$) and cell viability (CFU) as a function of time spent on a $0.2\times$ LB agar plate. At time zero, multiple plates were inoculated by spreading either WT or $\Delta rcsC$ cells on the surfaces. At the time points indicated, cells were collected from a plate by suspending them in 2 ml of $0.2\times$ LB liquid. The OD_{600} values of these suspensions were immediately measured and multiplied by the total suspension volume (2 ml) to determine the biomass ($OD_{600} \times ml$). These suspensions were then used for CFU assays. In the plot, the measured values were normalized by the value of WT at the first time point. Error bars represent standard deviation from two independent experiments. *p* value (from a T-test) of CFU at 38 h $= 0.028$. **B** The fraction of $\Delta rcsC$ cells as a function of time spent on a $0.2\times$ LB agar plate in a competition experiment. WT and $\Delta rcsC$ cells were mixed in equal ratio (based on OD_{600}). At time zero, multiple plates were inoculated with the mixed culture. At a time point indicated, cells were collected from a plate, and a CFU assay was performed as discussed above. The $\Delta rcsC$ strain carries a kanamycin resistance marker. In the CFU assay, we distinguished $\Delta rcsC$ from WT cells by plating the liquid suspensions on kanamycin and kanamycin-free LB plates (Supplemental Methods). Error bars represent the standard deviation from three independent experiments. We additionally performed similar competition experiments on agar plates with different agar concentrations (Supplementary Fig. 13).

the $\Delta rcsC$ strain exhibited a noticeably steeper decrease in cell viability than WT (Fig. 4A, upright and inverted triangles). When we characterized cell viability with propidium iodide (PI) staining, we observed a higher fraction of PI-stained cells in $\Delta rcsC$ than WT populations (Supplementary Fig. 12), which is in agreement with lower cell viability of $\Delta rcsC$ cells (Fig. 4A).

We next performed competition experiments to more directly compare their fitness. The WT and $\Delta rcsC$ strains were co-inoculated onto an agar surface in an equal ratio, and the cell viability of each strain was determined with a CFU assay over time (Supplementary Methods), and the fraction of $\Delta rcsC$ cells [= $N_{\Delta rcsC}$ / ($N_{\Delta rcsC} + N_{WT}$)] was calculated. We observed a decrease in the $\Delta rcsC$ fraction over time (Fig. 4B and Supplementary Fig. 13). These data collectively reveal a trade-off between population expansion and viability.

DISCUSSION

Our quantitative imaging uncovered intricate spatial dynamics of cell motility governing partial migration of a population. We then systematically analyzed the dynamics (colony center vs. edge, WT vs. Δrcs strains, high vs. low-nutrient levels on agar surface and in liquid culture), which revealed an important role of the Rcs system in these dynamics. The Rcs system is widespread in the *Enterobacteriaceae* family [49] and is known to regulate a wide range of cellular functions including capsular polysaccharide or colanic acid synthesis, cell envelope maintenance, cell division and virulence [50]. However, physiological cues inducing this system and its functional role in colonizing territories were unclear. Our present work reveals that nutrient-dependent repression of *flhDC* expression by the Rcs system leads to intricate dynamics of cell motility in an expanding population, thereby having a major impact on the surface colonization pattern.

Our work reveals a trade-off underlying population motility. Previous studies of evolution have shown that *E. coli* cells can increase their swimming speeds at the expense of cell growth [51, 52]. Hyper-swarming *Pseudomonas aeruginosa*, which moves faster than the parental strain, can be evolved but is outcompeted in biofilm formation [53]. Previous work has shown that swarming *P. mirabilis* cells are mechanically fragile and more susceptible to cell-wall stress [54]. Our finding on the fitness disadvantage of Δrcs is consistent with these studies. Furthermore, swimming in liquid costs about 2% of metabolic budget in bacteria [55]. Although the cost of surface motility (swarming) has not been measured, it is thought to be much greater [26, 56]. Consistent with this view, we found that *P. mirabilis* cells that are actively moving on a surface reproduce at a very low rate or do not reproduce (Supplementary Fig. 14), indicating a severe cost of surface motility. This cost is likely more burdensome in nutrient-limiting conditions, where cells already suffer from a limited metabolic budget. Our studies show that, although inducing migration in the face of this cost (Δrcs strain) does lead to faster population expansion, it severely impairs population fitness. Nutrient-dependent repression of cell motility by Rcs can minimize this cost in nutrient-limited cells while enabling migration only for a small number of privileged cells that have access to nutrients. This mode of partial migration can provide one mechanism to mediate a trade-off, helping a population maintain its fitness during expansion, thereby facilitating surface colonization.

Previous studies suggest an additional mechanism for fitness advantage. RpoS is a general stress sigma factor that is widely present in *Enterobacteriaceae* [57]. In our previous studies with *E. coli*, we have shown that in nutrient-limiting conditions, RpoS plays a critical role in conserving a limited metabolic budget for starvation survival [58]. Such a protective role of RpoS is well documented for a wide variety of other bacterial species [57]. Recent studies have found that RpoS expression is induced by Rcs [59, 60]. Therefore, Rcs not only represses cell motility in the nutrient-limited region (as discussed in the preceding paragraph) but also is expected to induce the expression of the important stress sigma factor (RpoS). This two-pronged response is likely to contribute to the fitness advantage conferred by Rcs. Importantly, migration is expected to incur a high cost of dispersal in other organisms as well, impairing their reproduction rate and survival

[61–63]. A similar strategy could be used in these organisms to optimize territory expansion.

Another important finding from other studies of *E. coli* is that *flhDC* expression is stimulated by nutrient limitation [64, 65] (possibly through cAMP-CRP [66–68]). A similar mechanism could explain a significant increase in *flhDC* expression at decreasing nutrient levels in the *P. mirabilis* $\Delta rcsC$ strain (Fig. 3A, C, red). The WT strain also exhibited an increase in *flhDC* expression (Fig. 3A, C, green). However, the increase in the WT strain was minor because Rcs-mediated *flhDC* repression became stronger and counteracted the stimulating effect of nutrient limitation on *flhDC* expression (Fig. 3B, D). This strategy ensures that cells in the colony center do not differentiate and swarm (Fig. 2), keeping the migratory subpopulation low.

Our colony images of the *flhDC-gfp* strain additionally illustrate the cell-to-cell variability in *flhDC* expression. GFP-bright cells, which eventually differentiate and swarm, are preferentially located at the colony edge in the WT strain, but not all cells at the edge are GFP-bright (Fig. 2A). In the $\Delta rcsC$ colony, GFP-bright cells are located throughout the colony, but again, not all cells are GFP-bright (Fig. 2A). This cell-to-cell variability can be explained by our previous finding that FlhDC auto-activates its expression [30]. This auto-activation is an example of positive feedback, which is known to generate bi-stability, i.e., two distinct levels of gene expression [69]. Positive feedback is shown to be a common mechanism for biological systems exhibiting differentiation [69]. Studies have found that positive feedback, coupled with the stochastic gene expression noise, triggers a fraction of a population to differentiate [70]. If the expression of a key regulator stochastically exceeds a threshold value, positive feedback drives the expression to even higher levels, triggering differentiation. In the $\Delta rcsC$ strain, without Rcs-mediated repression, the baseline of *flhDC* expression is higher, making it easier to exceed the threshold value. Therefore, a higher fraction of cells differentiates and contributes to rapid colony expansion.

Our findings also shed new light on a type of surface-attached microbial community, biofilm. Surface motility is known to have a dramatic effect on biofilm formation [27, 53]. We found that motility is strongly repressed by Rcs in a dense region of a colony (Fig. 2A), which ensures that a majority of cells remain sessile within the colony. Due to this repression, the boundary of a parental colony remains distinct and stationary during expansion (Fig. 1A), which enables the maintenance of the original densely-packed community. The same mechanism is likely at play in a biofilm, where Rcs ensures the formation of a robust biofilm by inhibiting premature dispersal. This is consistent with previous studies of *E. coli, P. mirabilis*, and other bacteria, which have shown that *rcs* deletion leads to the formation of defective biofilms [38, 71, 72].

REFERENCES

1. Flemming H-C, Wingender J, Szewzyk U, Steinberg P, Rice SA, Kjelleberg S. Biofilms: an emergent form of bacterial life. Nat Rev Microbiol. 2016;14:563–75.
2. Nadell CD, Xavier JB, Foster KR. The sociobiology of biofilms. FEMS Microbiol Rev. 2009;33:206–24.
3. Rumbaugh KP, Sauer K. Biofilm dispersion. Nat Rev Microbiol. 2020;18:571–86.
4. Costerton JW, Stewart PS, Greenberg EP. Bacterial biofilms: a common cause of persistent infections. Science. 1999;284:1318–22.
5. Drenkard E, Ausubel FM. Pseudomonas biofilm formation and antibiotic resistance are linked to phenotypic variation. Nature. 2002;416:740–3.
6. de Carvalho CCCR. Marine biofilms: a successful microbial strategy with economic implications. Front Mar Sci. 2018;5:126.
7. McDougald D, Rice SA, Barraud N, Steinberg PD, Kjelleberg S. Should we stay or should we go: mechanisms and ecological consequences for biofilm dispersal. Nat Rev Microbiol. 2012;10:39–50.
8. Nathan R, Getz WM, Revilla E, Holyoak M, Kadmon R, Saltz D, et al. A movement ecology paradigm for unifying organismal movement research. Proc Natl Acad Sci USA. 2008;105:19052–9.

9. Yan J, Monaco H, Xavier JB. The ultimate guide to bacterial swarming: an experimental model to study the evolution of cooperative behavior. Annu Rev Microbiol. 2019;73:293–312.

10. Gokhale S, Conwill A, Ranjan T, Gore J. Migration alters oscillatory dynamics and promotes survival in connected bacterial populations. Nat Commun. 2018;9:5273.

11. Hallatschek O, Fisher DS. Acceleration of evolutionary spread by long-range dispersal. Proc Natl Acad Sci USA. 2014;111:E4911–9.

12. Birzu G, Hallatschek O, Korolev KS. Fluctuations uncover a distinct class of traveling waves. Proc Natl Acad Sci USA. 2018;115:E3645–54.

13. Ping D, Wang T, Fraebel DT, Maslov S, Sneppen K, Kuehn S. Hitchhiking, collapse, and contingency in phage infections of migrating bacterial populations. ISME J. 2020;14:2007–18.

14. Chen L, Noorbakhsh J, Adams RM, Samaniego-Evans J, Agollah G, Nevozhay D, et al. Two-dimensionality of yeast colony expansion accompanied by pattern formation. PLoS Comput Biol. 2014;10:e1003979.

15. Patra P, Kissoon K, Cornejo I, Kaplan HB, Igoshin OA. Colony expansion of socially motile Myxococcus xanthus cells is driven by growth, motility, and exopolysaccharide production. PLoS Comput Biol. 2016;12:e1005010.

16. Chapman BB, Brönmark C, Nilsson J-Å, Hansson L-A. The ecology and evolution of partial migration. Oikos. 2011;120:1764–75.

17. Lundberg P. Partial bird migration and evolutionarily stable strategies. J Theor Biol. 1987;125:351–60.

18. Kokko H. Directions in modelling partial migration: how adaptation can cause a population decline and why the rules of territory acquisition matter. Oikos. 2011;120:1826–37.

19. Singh NJ, Leonardsson K. Partial migration and transient coexistence of migrants and residents in animal populations. PloS One. 2014;9:e94750.

20. Armbruster CE, Mobley HLT. Merging mythology and morphology: the multifaceted lifestyle of Proteus mirabilis. Nat Rev Microbiol. 2012;10:743.

21. Schaffer JN, Pearson MM. Proteus mirabilis and urinary tract infections. Microbiol Spectr. 2015;3. https://doi.org/10.1128/microbiolspec.UTI-0017-2013.

22. Jones BV, Young R, Mahenthiralingam E, Stickler DJ. Ultrastructure of Proteus mirabilis swarmer cell rafts and role of swarming in catheter-associated urinary tract infection. Infect Immun. 2004;72:3941–50.

23. Li X, Zhao H, Lockatell CV, Drachenberg CB, Johnson DE, Mobley HL. Visualization of Proteus mirabilis within the matrix of urease-induced bladder stones during experimental urinary tract infection. Infect Immun. 2002;70:389–94.

24. Stickler DJ. Bacterial biofilms in patients with indwelling urinary catheters. Nat Clin Pr Urol. 2008;5:598–608.

25. Jacobsen SM, Stickler DJ, Mobley HLT, Shirtliff ME. Complicated catheter-associated urinary tract infections due to Escherichia coli and Proteus mirabilis. Clin Microbiol Rev. 2008;21:26–59.

26. Harshey RM. Bacterial motility on a surface: many ways to a common goal. Annu Rev Microbiol. 2003;57:249–73.

27. Verstraeten N, Braeken K, Debkumari B, Fauvart M, Fransaer J, Vermant J, et al. Living on a surface: swarming and biofilm formation. Trends Microbiol. 2008;16:496–506.

28. Kearns DB. A field guide to bacterial swarming motility. Nat Rev Microbiol. 2010;8:634–44.

29. Wu Y, Jiang Y, Kaiser AD, Alber M. Self-organization in bacterial swarming: lessons from myxobacteria. Phys Biol. 2011;8:055003.

30. Howery KE, Şimşek E, Kim M, Rather PN. Positive autoregulation of the flhDC operon in Proteus mirabilis. Res Microbiol. 2018;169:199–204.

31. Little K, Austerman J, Zheng J, Gibbs KA. Cell shape and population migration are distinct steps of Proteus mirabilis swarming that are decoupled on high-percentage agar. J Bacteriol. 2019;201:e00726–18.

32. Furness RB, Fraser GM, Hay NA, Hughes C. Negative feedback from a Proteus class II flagellum export defect to the flhDC master operon controlling cell division and flagellum assembly. J Bacteriol. 1997;179:5585–8.

33. Claret L, Hughes C. Functions of the subunits in the FlhD(2)C(2) transcriptional master regulator of bacterial flagellum biogenesis and swarming. J Mol Biol. 2000;303:467–78.

34. Deegan RD, Bakajin O, Dupont TF, Huber G, Nagel SR, Witten TA. Capillary flow as the cause of ring stains from dried liquid drops. Nature. 1997;389:827–9.

35. Andac T, Weigmann P, Velu SKP, Pinçe E, Volpe G, Volpe G, et al. Active matter alters the growth dynamics of coffee rings. Soft Matter. 2019;15:1488–96.

36. Nellimoottil TT, Rao PN, Ghosh SS, Chattopadhyay A. Evaporation-induced patterns from droplets containing motile and nonmotile bacteria. Langmuir. 2007;23:8655–8.

37. Clemmer KM, Rather PN. Regulation of flhDC expression in Proteus mirabilis. Res Microbiol. 2007;158:295–302.

38. Howery KE, Clemmer KM, Rather PN. The Rcs regulon in Proteus mirabilis: implications for motility, biofilm formation, and virulence. Curr Genet. 2016;62:775–89.

39. Howery KE, Clemmer KM, Şimşek E, Kim M, Rather PN. Regulation of the min cell division inhibition complex by the Rcs phosphorelay in Proteus mirabilis. J Bacteriol. 2015;197:2499–507.

40. Wang Q, Zhao Y, McClelland M, Harshey RM. The RcsCDB signaling system and swarming motility in Salmonella enterica Serovar Typhimurium: dual regulation of flagellar and SPI-2 virulence genes. J Bacteriol. 2007;189:8447–57.

41. Samanta P, Clark ER, Knutson K, Horne SM, Prüß BM. OmpR and RcsB abolish temporal and spatial changes in expression of flhD in Escherichia coli biofilm. BMC Microbiol. 2013;13:182.

42. Girgis HS, Liu Y, Ryu WS, Tavazoie S. A comprehensive genetic characterization of bacterial motility. PLoS Genet. 2007;3:e154.

43. Francez-Charlot A, Laugel B, Van Gemert A, Dubarry N, Wiorowski F, Castanié-Cornet MP, et al. RcsCDB His-Asp phosphorelay system negatively regulates the flhDC operon in Escherichia coli. Mol Microbiol. 2003;49:823–32.

44. Rieck VT, Palumbo SA, Witter LD. Glucose availability and the growth rate of colonies of Pseudomonas fluorescens. J Gen Microbiol. 1973;74:1–8.

45. Shao X, Mugler A, Kim J, Jeong HJ, Levin BR, Nemenman I. Growth of bacteria in 3-d colonies. PLoS Comput Biol. 2017;13:e1005679.

46. Warren MR, Sun H, Yan Y, Cremer J, Li B, Hwa T. Spatiotemporal establishment of dense bacterial colonies growing on hard agar. Elife. 2019;8:e41093.

47. Lavrentovich MO, Koschwanez JH, Nelson DR. Nutrient shielding in clusters of cells. Phys Rev E Stat Nonlin Soft Matter Phys. 2013;87:062703. -

48. Dal Co A, van Vliet S, Ackermann M. Emergent microscale gradients give rise to metabolic cross-feeding and antibiotic tolerance in clonal bacterial populations. Philos Trans R Soc Lond B Biol Sci. 2019;374:20190080.

49. Huang YH, Ferrières L, Clarke DJ. The role of the Rcs phosphorelay in Enterobacteriaceae. Res Microbiol. 2006;157:206–12.

50. Majdalani N, Gottesman S. The Rcs phosphorelay: a complex signal transduction system. Annu Rev Microbiol. 2005;59:379–405.

51. Fraebel DT, Mickalide H, Schnitkey D, Merritt J, Kuhlman TE, Kuehn S. Environment determines evolutionary trajectory in a constrained phenotypic space. Elife. 2017;6:e24669.

52. Yi X, Dean AM. Phenotypic plasticity as an adaptation to a functional trade-off. Elife. 2016;5:e19307.

53. van Ditmarsch D, Boyle KE, Sakhtah H, Oyler JE, Nadell CD, Déziel É, et al. Convergent evolution of hyperswarming leads to impaired biofilm formation in pathogenic bacteria. Cell Rep. 2013;4:697–708.

54. Auer GK, Oliver PM, Rajendram M, Lin T-Y, Yao Q, Jensen GJ, et al. Bacterial swarming reduces Proteus mirabilis and Vibrio parahaemolyticus cell stiffness and increases β-Lactam susceptibility. mBio. 2019;10:e00210–19.

55. Kaiser D. Bacterial swarming: a re-examination of cell-movement patterns. Curr Biol. 2007;17:R561–R70.

56. Inoue T, Shingaki R, Hirose S, Waki K, Mori H, Fukui K. Genome-wide screening of genes required for swarming motility in Escherichia coli K-12. J Bacteriol. 2007;189:950–7.

57. Dong T, Joyce C, Schellhorn H. The role of RpoS in bacterial adaptation. In: El-Sharoud W, editor. Bacterial physiology. Heidelberg: Springer, Berlin; 2008. pp 313-37.

58. Phaiboun A, Zhang Y, Park B, Kim M. Survival kinetics of starving bacteria is biphasic and density-dependent. PLoS Comput Biol. 2015;11:e1004198.

59. Majdalani N, Hernandez D, Gottesman S. Regulation and mode of action of the second small RNA activator of RpoS translation, RprA. Mol Microbiol. 2002;46:813–26.

60. Peterson CN, Carabetta VJ, Chowdhury T, Silhavy TJ. LrhA regulates rpoS translation in response to the Rcs phosphorelay system in Escherichia coli. J Bacteriol. 2006;188:3175–81.

61. Lok T, Overdijk O, Piersma T. The cost of migration: spoonbills suffer higher mortality during trans-Saharan spring migrations only. Biol Lett. 2015;11:20140944.

62. Flack A, Fiedler W, Blas J, Pokrovsky I, Kaatz M, Mitropolsky M, et al. Costs of migratory decisions: a comparison across eight white stork populations. Sci Adv. 2016;2:e1500931.

63. Rankin MA, Burchsted JCA. The cost of migration in insects. Annu Rev Entomol. 1992;37:533–59.

64. Ni B, Colin R, Link H, Endres RG, Sourjik V. Growth-rate dependent resource investment in bacterial motile behavior quantitatively follows potential benefit of chemotaxis. Proc Natl Acad Sci USA. 2020;117:595–601.

65. Amsler CD, Cho M, Matsumura P. Multiple factors underlying the maximum motility of Escherichia coli as cultures enter post-exponential growth. J Bacteriol. 1993;175:6238–44.

66. Yokota T, Gots JS. Requirement of adenosine 3', 5'-cyclic phosphate for flagella formation in Escherichia coli and Salmonella typhimurium. J Bacteriol. 1970;103:513–6.

67. Soutourina O, Kolb A, Krin E, Laurent-Winter C, Rimsky S, Danchin A, et al. Multiple control of flagellum biosynthesis in Escherichia coli: role of H-NS protein and the cyclic AMP-catabolite activator protein complex in transcription of the flhDC master operon. J Bacteriol. 1999;181:7500–8.

68. Silverman M, Simon M. Characterization of Escherichia coli flagellar mutants that are insensitive to catabolite repression. J Bacteriol. 1974;120:1196–203.

69. Mitrophanov AY, Groisman EA. Positive feedback in cellular control systems. Bioessays. 2008;30:542–55.
70. Raj A, van Oudenaarden A. Nature, nurture, or chance: stochastic gene expression and its consequences. Cell. 2008;135:216–26.
71. Ferrières L, Clarke DJ. The RcsC sensor kinase is required for normal biofilm formation in Escherichia coli K-12 and controls the expression of a regulon in response to growth on a solid surface. Mol Microbiol. 2003;50:1665–82.
72. Guttenplan SB, Kearns DB. Regulation of flagellar motility during biofilm formation. FEMS Microbiol Rev. 2013;37:849–71.

AUTHOR CONTRIBUTIONS
EŞ and MK conceived the study. EŞ and ED designed the experiments, analyzed and interpreted the data. EŞ and PR constructed strains. EŞ, ED and MK wrote the manuscript. All authors read and approved the manuscript.

COMPETING INTERESTS
The authors declare no competing interests.

ADDITIONAL INFORMATION
Supplementary information The online version contains supplementary material available at https://doi.org/10.1038/s41396-021-01148-w.

Correspondence and requests for materials should be addressed to Minsu Kim.

Reprints and permission information is available at http://www.nature.com/reprints

Publisher's note Springer Nature remains neutral with regard to jurisdictional claims in published maps and institutional affiliations.